COAL CHAR KINETICS OF OXIDATION AND GASIFICATION REACTIONS

Robert Lewtak[*], Jarosław Hercog

Institute of Power Engineering, Thermal Processes Department, Augustówka 36, 02-981 Warsaw, Poland

Experimental investigations and numerical simulations have been conducted in this study to derive and test the values of kinetic parameters describing oxidation and gasification reactions between char carbon and O_2 and CO_2 occurring at standard air and oxy-fuel combustion conditions. Experiments were carried out in an electrically heated drop-tube at heating rates comparable to full-scale pulverized fuel combustion chambers. Values of the kinetic parameters, obtained by minimization of the difference between the experimental and modeled values of char burnout, have been derived and CFD simulations reproducing the experimental conditions of the drop tube furnace confirmed proper agreement between numerical and experimental char burnout.

Keywords: kinetic parameters, char particle oxidation and gasification, oxy-fuel combustion

1. INTRODUCTION

From the three main groups of the CCS technologies, oxy–fuel combustion seems to be the most promising one due to the lowest energy penalty associated with the investment and operational costs (Jenni et al., 2013). The main feature of this technology is the combustion of fuel in the mixture of recycled flue gases and O_2. However, diluents present in a combustion system, such as CO_2 and H_2O, have different physical and chemical properties than N_2 present in air (Chen et al., 2012), which changes the particle temperature, heat transfer, emissions and char burnout (Toftegaard, 2010).

Rathnam et al. (2009) conducted oxy-fuel combustion tests in a DTF and reactivity analysis in TGA of four Australian coals. They found that the influence of CO_2 on coal burnout is coal dependent but in general the burnout was higher or similar in oxy-fuel conditions compared to air-combustion, which was attributed to higher char reactivity in the oxy-fuel atmosphere due to char–CO_2 reaction. Chars formed during pyrolysis experiments in pure CO_2 exhibited higher specific surface area in comparison to chars produced in N_2, which can also catalyse the surface reactions (Al-Makhadmeh, 2009; Rathnam et al., 2009). On the other hand, Brix et al. (2010) observed no significant differences in volatile yield or specific surface between chars produced in CO_2 and N_2 explaining this effect with shorter particle residence times than in previous study, which prevented char gasification reaction from occuring. Additionally, as the char combustion is concerned, Brix et al. (2010) observed no apparent difference between combustion in CO_2/O_2 and N_2/O_2 atmospheres. This result was also confirmed in a study of Maffei et al. (2013), where experiments of the single particle combustion of two, different rank coals have been conducted in a DTF in quiescent gas conditions in which longer particle burnout times and lower surface temperatures in CO_2/O_2 mixtures were observed. One should note though that the oxygen concentrations varied between 21 and 100% in the bulk gas, and the oxygen diffusivity in CO_2 lower

---

*Corresponding author, e-mail: robert.lewtak@ien.com.pl

than that in N_2 mixtures may have played a significant role. On the other hand, Gonzalo–Tirado et al. (2012) found that, at low oxygen concentrations, the contribution of gasification with CO_2 to the overall rate can compensate for the change of the atmosphere and oxy-fuel combustion results in a slightly enhanced consumption rate with respect to char oxidation in air.

Thus, there is still a requirement for comprehensive studies of coal char combustion in air and oxy-fuel combustion conditions at scales comparable to pulverized fuel boilers. Moreover, it is necessary to address the changed combustion mechanism in oxy–fuel modeling since both oxidation and gasification reactions take place in parallel. It is also important to note that there is no fully convincing experimental evidence about the real reaction path, especially when models of different complexity are available that are often contradictory to each other (Hurt, et al., 2001).

In this study, experimental data, achieved in a number of tests carried out in a DTF, were used to derive a set of most adequate kinetic parameters of oxidation and gasification reactions applicable to numerical simulations of the oxy–fuel combustion process in pulverized fuel boilers.

2. EXPERIMENTAL SETUP

Experiments of pulverized coal char combustion have been carried out in a 6–meter drop tube, presented in Fig. 1, with 38.5 mm of inner diameter, in operating conditions similar to full scale combustion furnaces, i.e. the gas reactor temperature ranging from 900 to 1300 °C, oxygen mole fractions from 3 to 9% in CO_2 or N_2 diluents and residence time up to 1.2 s. All gas flows were adjusted using mass flow controllers in order to maintain the required atmosphere composition and particle residence times. Reactor wall temperatures were controlled by S-type thermocouples measuring the outer surface of the tube, while the reactor gas temperature was measured by the suction pyrometer inserted through one of the horizontal ports. Wall temperatures were adjusted accordingly to maintain the desired gas temperatures inside the reactor.
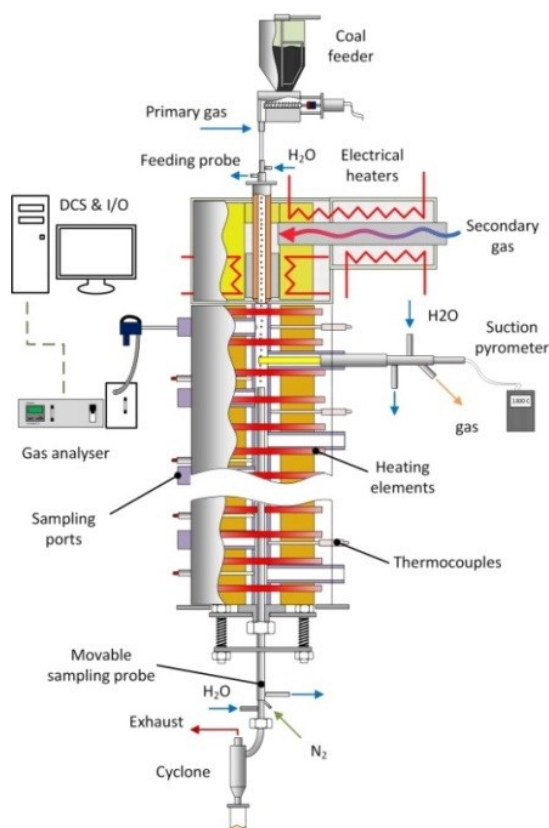

Fig. 1. Schematic of char combustion facility

Char particles were pneumatically fed into the reactor using a precise screw feeder and a water-cooled probe through one of the twelve, sloped ports installed along the reactor height. The particle mass flow was adjusted before starting of the test to hinder the concentration changes of the reaction gases (CO_2 and O_2) of more than 10%. That ensured virtually constant bulk gas compositions during the experiments. Changing the position of the feeding probe while the collection point remained stationary varied the particle residence time. Char burnout, X_C, was determined using the ash tracer method and calculated with the following formula:

$$X_C = \frac{f_a - f_{a,0}}{f_a\left(1 - f_{a,0}\right)}.$$ (1)

Char, from bituminous coal, screened between 63 and 90 μm, was produced at high heating rate of $10^4 - 10^5$ K/s and reactor temperature of 1300 °C, either in pure CO_2 or N_2 for oxy-fuel or air combustion, respectively, although coal devolatilization usually proceeds with small O_2 amount in industrial coal-burning installations. The residence time of devolatilization was set up to 250 ms ensuring complete devolatilization and preventing extensive gasification in case of oxy–fuel devolatilization (some gasification level could be nevertheless observed). The properties of the parent fuel and resulting chars are collected in Table 1. It is worth noting there is a difference of carbon content in char devolatilized in CO_2 and N_2 that indeed influences the burning time but has no effect on the combustion rate. Fig. 2 shows particle volume distributions measured with a Kamika 2DiSA instrument.

Table 1. Parent fuel and char properties

properties	raw coal	CO_2 char	N_2 char
moisture, %wt. ab	8.80	1.30	1.22
ash, %wt. db	11.62	28.23	21.89
volatiles, %wt. db	38.60	0.91	1.11
C, %wt. db	70.50	69.10	75.52
H, %wt. db	4.88	0.34	0.32
N, %wt. db	1.36	1.48	1.53
S, %wt. db	0.49	0.49	0.43
O, %wt. db, diff	11.14	0.36	0.32

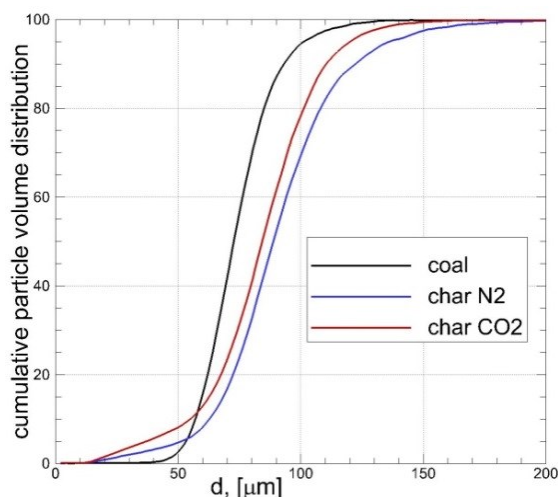ab-analytical basis, db-dry basis, diff-calculated by difference

Fig. 2. Cumulative particle volume distribution of coal and chars

3. DESCRIPTION OF THE CHAR COMBUSTION MODEL

When pulverized char particles are burnt in oxy-fuel conditions, besides oxidation, the combustion mechanism additionally takes into account the gasification by CO_2. Here, the single film-model (Caram et al., 1977), widely used to describe char oxidation, is also used here to describe gasification. Similar to O_2, it is assumed that CO_2 diffuses to the char particle surface where it reacts to form CO which then diffuses outward the particle surface without oxidation (Caram et al., 1977; Fendell, 1969; Mitchell, 1987). For the oxidation reaction, the production of CO_2 can be assumed to be negligible at high temperatures so that CO is the primary product of char carbon oxidation (Shaddix et al., 2013). Moreover, the homogeneous reaction of CO oxidation is not considered in the model while its thermal effect can further affect the combustion process. Thus, the combustion mechanism of char carbon is composed of two surface reactions as follows:

$$C + \tfrac{1}{2} O_2 \rightarrow CO, \tag{2}$$

$$C + CO_2 \rightarrow 2CO. \tag{3}$$

The total rate of char carbon consumption, r_C, is defined as follows:

$$r_C = \sum_{i=1}^{i=2} r_{C,i} \tag{4}$$

where i denotes the i-th surface reaction, and

$$r_{C,1} = A_p f(X_C) M_C \psi_1 \frac{k_{c,1} k_d}{k_d + k_{c,1} f(X_C)} C_{O_2,\infty} \tag{5}$$

since both diffusion and kinetics can affect the oxidation rate, and

$$r_{C,2} = A_p f(X_C) M_C \psi_2 k_{c,2} C_{CO_2,\infty} \tag{6}$$

since the rate of the gasification reaction is limited only by the char chemical reactivity, and $\psi_1 = 2$ mol-C/mol-O_2, $\psi_2 = 1$ mol-C/mol-CO_2, $C_{O_2,\infty}$ is the g-th species concentration in the bulk flow, $M_C = 12$ kg/kmol. The individual reaction rates, $r_{C,i}$ are expressed in terms of the external particle surface $A_p = \pi d_p^2$ so that the current model of char combustion belongs to a family of global char combustion models (Smith, 1982; Smith et al., 1994; Wall, 1986) unlike to intrinsic modeling approach considering development of the internal structure inside the fuel particle. The rate coefficient of the i-th surface reaction is expressed in the form of the Arrhenius equation

$$k_{c,i} = A_i e^{-E_i/(RT_s)} \tag{7}$$

in which A_i and E_i are the kinetic parameters. The mass transfer coefficient is defined as

$$k_d = \frac{Sh\, D}{d_p} \tag{8}$$

in which Sh is the Sherwood number, and the effective diffusion coefficient is expressed as

$$D(T, p) = D_0 \left(\frac{T_f + T_p}{2T_0} \right)^{1.75} \frac{p_0}{p} \tag{9}$$

where $D_0 = D_{O2-N2} = 0.181$ cm²/s at $T_0 = 273$ K and $p_0 = 1$ bar (Maloney, 2008) was used in O_2/N_2 combustion, while $D_0 = 0.154$ cm²/s was used in O_2/CO_2 combustion, and

$$f(X_C) = (1 - X_C(t))^q \tag{10}$$

is the correction function which takes into account the development of the specific surface area and the effect of the non–reactive ash surface during the particle combustion (Haas et al., 1997; Baum et al., 1971).

Finally, the governing equations of the char combustion model can be presented. Gas phase is treated in the Eulerian approach and coal particles are treated as Lagrange discrete particles whose mass and temperature evolution is described by equations given below. It was assumed that the particle volume, $V_p = \frac{\pi}{6} d_p^3$, is constant during combustion so that the mass conservation law of the char particle is expressed in the following form:

$$V_p \frac{d\rho_p}{dt} = -r_C(t) , \quad \rho_p(0) = \rho_{p,0} \tag{11}$$

and the char particle mass is then defined as

$$m_p(t) = m_a + m_C(t) \tag{12}$$

in which

$$m_a = f_{a,0}\, \rho_{p,0}\, V_p \tag{13}$$

is constant mass of ash contained in the char particle.

The char particle temperature, T_p, is defined by the conservation law of particle energy as follows (Lewtak et al., 2013):

$$m_p(t) c_p \frac{dT_p(t)}{dt} = h^* A_p \left(T_{f,\infty} - T_p(t)\right) + A_p \varepsilon_p \sigma \left(T_{f,\infty}^4 - T_p^4(t)\right) + \sum_{i-1}^{i=2} r_{C,i}(t)\Delta H_i \tag{14}$$

with the initial condition

$$T_p(t=0) = T_{p,0}, \tag{15}$$

where the heat transfer coefficient, h^*, corrected by the Ackermann correction, is defined as

$$h^* = \frac{k_{f,\infty}}{d_p} Nu \frac{\Phi}{e^\Phi - 1} \tag{16}$$

in which

$$\Phi = \frac{r_C}{2\pi\, d_p\, \rho_f\, D} \tag{17a}$$

is the non-dimensional heat transfer rate coefficient, and

$$Nu = 2 + 0.6 Re_p^{1/2} Pr^{1/3} \tag{17b}$$

is the Nusselt number.

Furthermore, in the current study, the partial oxidation of CO in the char particle boundary layer is taken into consideration by the modification of the heat released during coal char oxidation as follows

$$\Delta H_1 = (1-\chi)H_{CO} + \chi H_{CO_2} \tag{18}$$

where $\chi \in \langle 0,1 \rangle$ and $H_{CO} = 9.21$ MJ/kg-C, $H_{CO2} = 32.8$ MJ/kg-C while $\Delta H_2 = -4.3$ MJ/kg-C for the gasification reaction. Moreover, it should be also noted that CO oxidation influences the char combustion rate by the additional heat release and by O_2 consumption reducing its availability (reducing its flow to the particle surface). In addition, CO oxidation is negligible even at a surface temperature as high as 2500 K when water and hydrogen are absent (Goel et al., 1996).

4. RESULTS AND DISCUSSION

The mathematical model describing combustion of a char particle is comprised of a set of two ordinary differential Eqs. (11) and (14) in which the optimal values of the model parameters, i.e. the kinetic parameters, A_i and E_i, and the q exponent, exist and satisfy

$$\min_{A_i, E_i, q} \sum_j \left| X_C^{num}(t_j) - X_C^{exp}(t_j) \right| \tag{19}$$

where j are numbers of all experimental points. The optimal values of A_i, E_i and q shown in Table 2 have been determined by the generalized reduced gradient method (Lasdon et al., 1975) for which the fourth-order Runge-Kutta method was used to solve the system (11) and (14) to determine the values of X_C^{num}.

Table 2. Optimal values of the kinetic parameters and q

model	q	A_1 (m/s)	E_1 (kJ/mol)	A_2 (m/s)	E_2 (kJ/mol)
$\chi = 0$	1.65	6700	77.5	2.55×10^6	214
$\chi = 0.2$	1.65	5390	75.8	3.58×10^6	221
$\chi = 0.4$	1.65	3370	71.8	4.21×10^6	222

a) char burnout, X_C, for O_2/N_2

b) char burnout, X_C, for O_2/CO_2

c) char temperature, T_p, for O_2/N_2
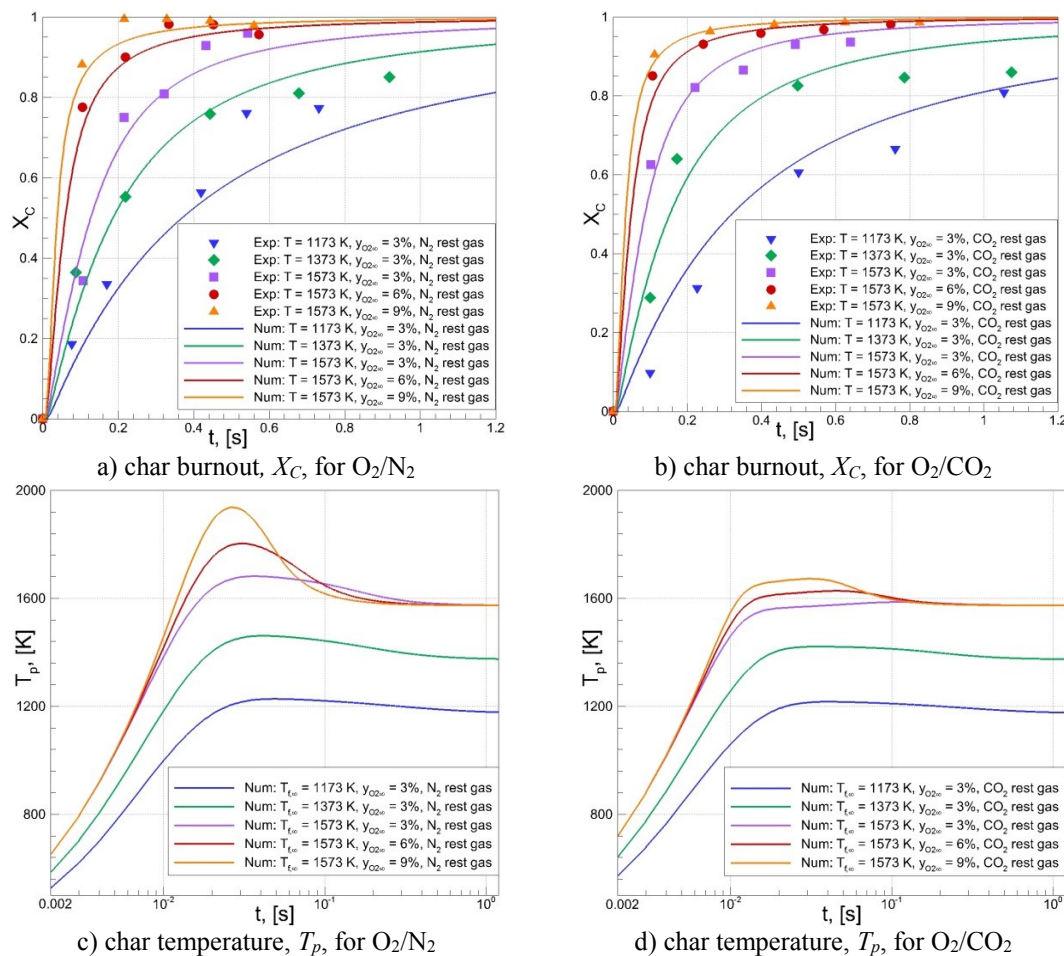
d) char temperature, T_p, for O_2/CO_2

Fig. 3. Char burnout and temperature. Solid lines represent a numerical solution of Eq. (11) and Eq. (14) without CO oxidation ($\chi = 0$) derived for the optimal values of the model parameters. Points represent X_C derived from experiments

As shown in Fig. 3, the numerical char burnout correctly reproduces the experimental results for both standard and oxy–fuel conditions. Moreover, the particle temperature predicted by the model shows different behavior for O_2/N_2 that in O_2/CO_2. For standard combustion in O_2/N_2 mixtures, the particle temperature curves show steep slopes with the in–between temperature peak, especially visible for high gas temperature and concentrations of O_2. For the oxy-fuel conditions, the particle temperature curves are flat with no temperature peaks due to the active endothermic gasification reaction. One can also note that the ratio between burnouts in oxy-fuel and air conditions changes with the temperature and oxygen concentration. At lower temperatures (900 °C) and low oxygen mole fraction (3 %), the burnouts in oxy-fuel and air are similar due to the low effect of the gasification reaction. At higher temperatures (1100 and 1300 °C) and low oxygen mole fraction (3 %), the burnouts in oxy-fuel are higher than in air since the gasification rate increases and contributes significantly to the overall burnout. At high temperature (1300 °C) and moderate oxygen mole fraction (6 %), the burnouts in oxy-fuel and air are again comparable because the oxidation rate increases and the effect of oxygen diffusion to the particle surface starts to play a role. Finally, at high temperature (1300 °C) and higher oxygen mole fraction (9 %), the burnout in oxy-fuel is lower than in air due to the significant effect of the oxygen diffusion. Thus, it is important to take into account the influence of the gasification reaction and oxygen diffusion in mathematical modeling of oxy-fuel combustion in practical combustion systems.

The mathematical model of char particle combustion described above has been implemented in ANSYS Fluent to simulate the experimental drop-tube furnace conditions and test the values of the kinetic parameters already derived.

Figure 4 shows the evolution of char burnout and particle temperature for char burnt in standard and oxy-fuel conditions. Experimental char burnout shown as points has been compared with the numerical solution of Eq. (11) and Eq. (14) carried out for the optimal values of the model parameters presented in Table 2 without CO oxidation in the particle boundary layer ($\chi = 0$). Additionally, Table 2 presents the optimal model parameters when partial oxidation of CO in the particle boundary layer is taken into consideration, i.e. selected for $\chi = 0.2$ and $\chi = 0.4$. It can be observed that the effect of CO partial oxidation on the kinetic parameters mainly affects values of the pre-exponential factors while values of the activation energies remain nearly constant. Numerical optimization has been carried out for average char particle diameters equal to 69 μm for char produced in N_2, and 62 μm for char produced in CO_2. Additionally, particle emissivity and specific heat were assumed to be equal to 0.9 and 1680 J/(kg·K), respectively.

Fig. 4 shows selected contours of gas velocity and temperature, CO mole fraction and particle trajectories from the CFD modeling of coal char combustion in the drop-tube furnace. All CFD simulations have been carried out for pulverized coal char particles in a diameter range conformed with the experimental particle size distributions. Char particles which are immediately transported close to the hot wall of the drop-tube furnace heat up quicker than char particles flowing through the centre, where the gas temperature is lower, due to cold primary air introducing char particles.

Figure 5 shows the evolution of coal char burnout for oxy-fuel conditions derived from experimental and CFD investigations. The CFD lines plotted for all particle sizes considered in the CFD modeling create a family of lines limited by a top and bottom envelope. The experimental points are located near the top envelope of all CFD lines since the kinetic parameters have been derived assuming the ideal process conditions of constant gas temperature and constant gas concentrations during combustion of char particles. Meanwhile, the conditions of gas temperature and concentrations acting on the char particles were variable in CFD and experimental investigations have given a wide band of CFD char burnout. Moreover, the top envelope exactly represents the char burnout line achieved for the ideal conditions considered during optimization of the model parameters.
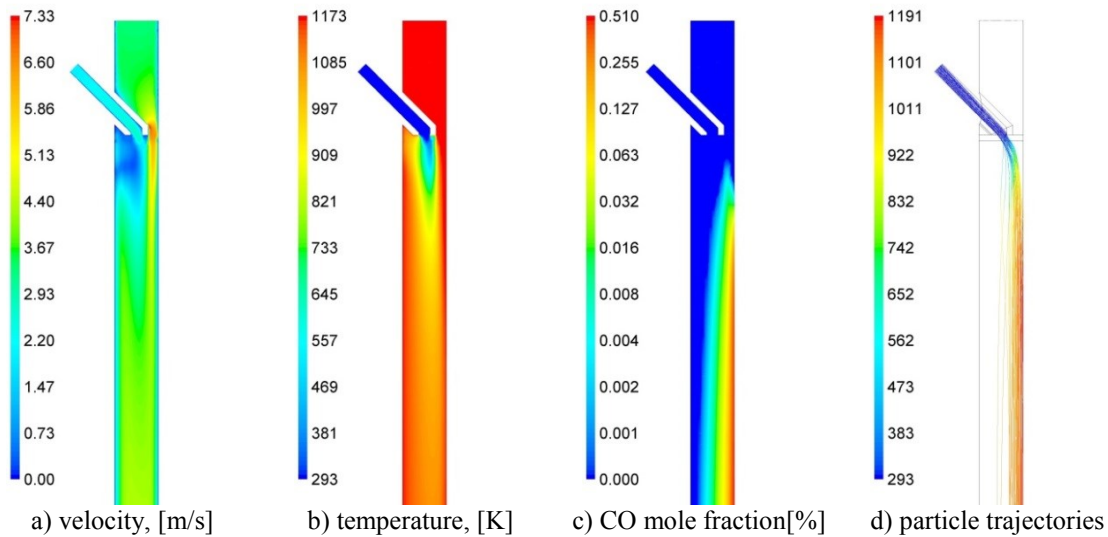
a) velocity, [m/s]   b) temperature, [K]   c) CO mole fraction[%]   d) particle trajectories

Fig. 4. Selected CFD modeling of pulverized char combustion in the drop tube furnace at oxy-fuel conditions of $T_{f,\infty} = 1173$ K, $y_{O2,\infty} = 3\%$. Particle trajectories, (d), coloured by particle temperature in K
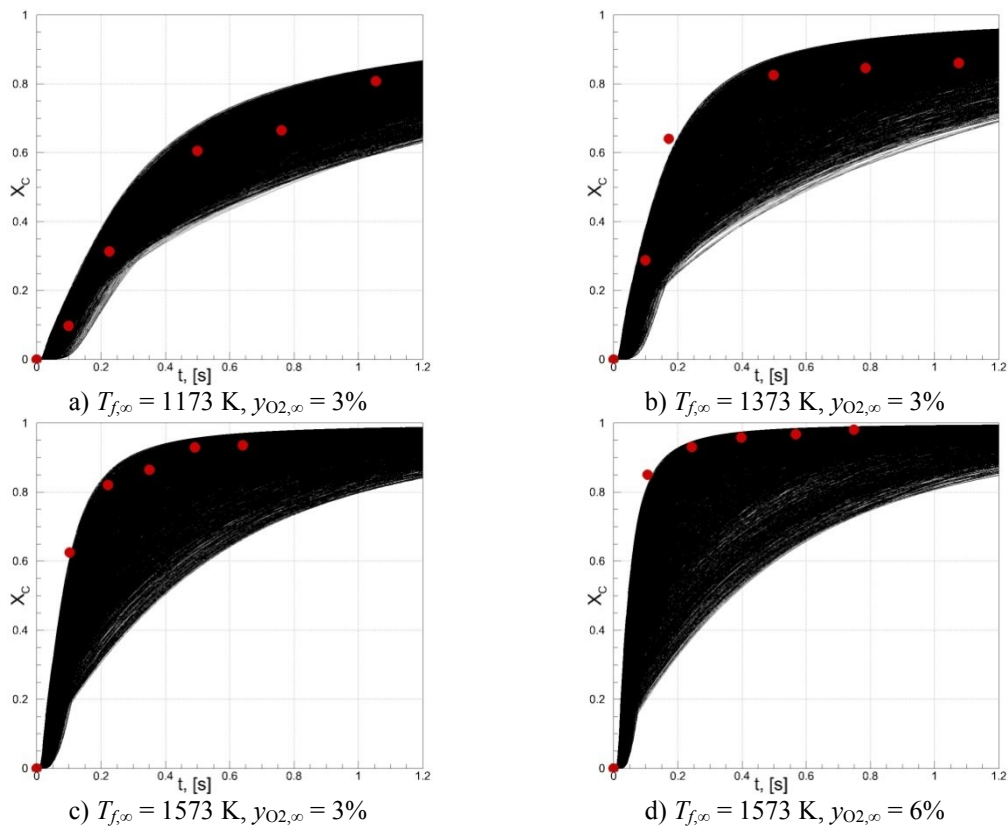

a) $T_{f,\infty} = 1173$ K, $y_{O2,\infty} = 3\%$

b) $T_{f,\infty} = 1373$ K, $y_{O2,\infty} = 3\%$

c) $T_{f,\infty} = 1573$ K, $y_{O2,\infty} = 3\%$

d) $T_{f,\infty} = 1573$ K, $y_{O2,\infty} = 6\%$

Fig. 5. Evolution of char burnout for oxy-fuel conditions (CO_2 as the rest gas),
— CFD solution,   ● experimental points

5. CONCLUDING REMARKS

The experimental investigations carried out in the current study revealed the influence of the combustion atmosphere on char burnout. It has been observed that when char particles are burnt in oxy-fuel conditions, i.e. at a high amount of CO_2 with low O_2 concentrations that is usually encountered in

oxy-fuel combustion chambers, gasification enhances char burnout so that its influence has to be taken into consideration although the oxidation process always plays the dominant role in combustion.

Next, to determine the values of kinetic parameters that describe the combustion process, both the experimental investigations and CFD simulations have been combined which turned out to be an attractive and well-posed approach to apply.

Numerical results, predicted by the mathematical model proposed here and describing char combustion in oxy-fuel conditions, are in proper agreement with experimental data. Thus, the approach presented here to derive kinetic parameters has been verified and the model can be applied to CFD simulations of pulverized fuel flames in oxy-fuel conditions.

SYMBOLS

A	pre-exponential factor , m/s, or surface area, m^2
c	specific heat, J/(kg K)
C	mole concentration, $kmol/m^3$
d	diameter, m
D	effective diffusion coefficient, cm^2/s
E	activation energy, kJ/mol
f	mass fraction
ΔH	heat of reaction, MJ/kg-C
m	mass, kg
M	molecular weight, kg/kmol
k_c	rate coefficient of a surface reaction, m/s
k_d	mass transfer coefficient, m/s
p	pressure, Pa
R	gas constant
r	rate of gas-solid reaction, kg/s
t	time, s
T	temperature, K
V	volume, m^3
X	burnout, non-dimensional

Greek symbols

ε	emissivity
ρ	density, kg/m^3
ψ	conversion factor, mol-C/mol-g
σ	Stefan–Boltzmann constant, $W/(m^2 K^4)$

Subscripts

0	initial or reference condition
a	ash
C	carbon
i	reaction index
g	gas

p   particle

∞   bulk flow condition

REFERENCES

Al-Makhadmeh L., 2009. *Coal pyrolysis and char combustion under oxy-fuel conditions*, PhD thesis, Stuttgart, Universität Stuttgart.

Baum M.M., Street P.J., 1971. Predicting the combustion behaviour of coal particles. *Combust. Sci. Technol*., 3 (5), 231-243. DOI: 10.1080/00102207108952290.

Brix J., Jensen P.A., Jensen A.D., 2010. Coal devolatilization and char conversion under suspension fired conditions in O_2/N_2 and O_2/CO_2 atmospheres. *Fuel,* 89, 3373–3380. DOI: 10.1016/j.fuel.2010.03.019.

Caram H.S., Amundson N.R., 1977. Diffusion and reaction in a stagnant boundary layer about a carbon particle. *Industrial & Engineering Chemistry Fundamentals*, 16 (2), 171–181. DOI: 10.1021/i160062a001.

Chen L., Yong S.Z., Ghoniem A.F., 2012. Oxy-fuel combustion of pulverized coal: Characterization, fundamentals, stabilization and CFD modeling. *Progress in Energy and Combustion Science*, 38, 156-214. DOI: 10.1016/j.pecs.2011.09.003.

Fendell F.E., 1969. The burning of spheres gasified by chemical attack. *Combust. Sci. Technol*., 1, 13–24. DOI: 10.1080/00102206908952188.

Goel S., Lee C.H., Longwell J.P., Sarofim A.F., 1996, Modelling of ignition and CO oxidation in the boundary layer of a single char particle, *Energy Fuels*, 10, 1091-1098. DOI: 10.1021/ef9502416.

Gonzalo–Tirado C., Jiménez S., Ballester J., 2012. Gasification of a pulverized subbituminous coal in CO_2 at atmospheric pressure in an entrained reactor. *Combust. Flame*, 159, 385 – 395. DOI: 10.1016/j.combustflame.2011.07.001.

Haas J.H.P., Maalman T., Gallagher G., van de Kamp W., 1997. Pulverized fuel combustion. Characterization of coal blends. *IFRF* Doc No F 37/y/38.

Hurt R., Calo J., 2001. Semi–global intrinsic kinetics for char combustion modelling. *Combust. Flame,* 125, 1138-1149. DOI: 10.1016/S0010-2180(01)00234-6.

Jenni K.E., Baker E.D., Nemet G.F., 2013. Expert elicitations of energy penalties for carbon capture technologies. *Int. J. Greenhouse Gas Control*, 12, 136–145. DOI: 10.1016/j.ijggc.2012.11.022.

Lasdon L.S., Waren A.D., Jain A., Ratner M., 1975. *Design and testing of a generalized reduced gradient code for nonlinear optimization*. USA, NTIS.

Lewtak R., Milewska A., 2013. Application of different diffusion approaches in oxy-fuel combustion of single coal char particles. *Fuel*, 113, 844-853. DOI: 10.1016/j.fuel.2013.01.053.

Maloney J.O., *Perry's chemical engineers' handbook*, McGraw-Hill; 2008.

Maffei T., Khatami R., Pierucci S., Faravelli T., Ranzi E., Levendis Y.A., 2013. Experimental and modeling study of single coal particle combustion in O_2/N_2 and Oxy-fuel (O_2/CO_2) atmospheres. *Combust. Flame*, 160, 2559-2572. DOI: 10.1016/j.combustflame.2013.06.002.

Mitchell R.E., 1987. Experimentally determined overall burning rates of coal chars. *Combust. Sci. Technol.*, 53, 165–186. DOI: 10.1080/00102208708947025.

Rathnam RK, Elliott LK, Wall TF, Liu Y, Moghtaderi B., 2009. Differences in reactivity of pulverised coal in air (O_2/N_2) and oxy-fuel (O_2/CO_2) conditions. *Fuel Process Technol*., 90, 797–802. DOI: 10.1016/j.fuproc.2009.02.009.

Shaddix C.R., Holzleithner F., Geier M., Haynes B.S., 2013. Numerical assessment of Tognotti determination of CO_2/CO production ratio during char oxidation. *Combust. Flame*, 160, 1827 – 1834. DOI: 10.1016/j.combustflame.2013.03.019.

Smith I.W., 1982. The combustion rates of coal chars: a review. *19th Int. Symposium on Combustion*, Technion-Israel Institute of Technology, Haifa, Israel, 8-13 August 1982, 1045-1065. DOI: 10.1016/S0082-0784(82)80281-6.

Smith K.L Smoot L.D., Fletcher T.H., Pugmire R.J., 1994. *The structure and reaction processes of coal*. The Plenum Chemical Engineering Series.

Toftegaard M.B., Brix J., Jensen P.A., Glarborg P., Jensen A.D., 2010. Oxy–fuel combustion of solid fuels. *Prog. Energy Combust. Sci.*, 36, 581–625. DOI: 10.1016/j.pecs.2010.02.001.

Wall T.F., Gururajan V.S., 1986. Combustion kinetics and the heterogeneous ignition of pulverized coal. *Combust. Flame*, 66, 151-157. DOI: 10.1016/0010-2180(86)90087-8.